INFLATION: THEORETICAL AND OBSERVATIONAL STATUS

Cosmic Inflation and Model Comparison
Quel est le Meilleur Modèle d'Inflation?

Vincent Vennin[a], Jérôme Martin [b], Christophe Ringeval[c]

[a] **Institute of Cosmology & Gravitation, University of Portsmouth,**
Dennis Sciama Building, Burnaby Road, Portsmouth, PO1 3FX, United Kingdom
E-mail: vincent.vennin@port.ac.uk
[b] **Institut d'Astrophysique de Paris, UMR 7095-CNRS,**
Université Pierre et Marie Curie, 98 bis boulevard Arago, 75014 Paris, France
E-mail: jmartin@iap.fr
[c] **Centre for Cosmology, Particle Physics and Phenomenology,**
Institute of Mathematics and Physics, Louvain University,
2 Chemin du Cyclotron, 1348 Louvain-la-Neuve, Belgium
E-mail: christophe.ringeval@uclouvain.be

Abstract. We analyze the implications for inflation of the recently released Planck Cosmic Microwave Background data and explain why the single-field slow-roll scenarios with minimal kinetic terms are favored. Within this class of models, we show how Bayesian model comparison can be used to further exclude about one third of the inflationary scenarios. We also study the end of inflation and show that Planck can already constrain the reheating phase. Finally, we conclude by discussing how future missions will be able to improve our knowledge of the inflationary mechanism.

Nous discutons les implications pour l'inflation des données récemment obtenues par le satellite Planck. Nous expliquons pourquoi les scenarios à un champs scalaire et terme cinétique standard, dans le régime de roulement lent, sont favorisés. À l'intérieur de cette classe de modèles, nous montrons comment l'approche Bayésienne peut être utilisée pour identifier les scénarios les plus plausibles et contraindre la fin de l'inflation et la phase de réchauffement. Nous concluons en discutant comment de futures missions spatiales nous permettrons d'améliorer notre connaissance de l'inflation.

Cosmology/ Inflation/ Model Comparison

1. Introduction

Cosmic inflation [1, 2, 3, 4, 5] is an attempt to describe the physical conditions that prevailed in the very early Universe. It consists in a phase of accelerated expansion that took place at very high energy, before the hot Big Bang era. As a consequence, the initial conditions for standard cosmology are in fact determined by what happened during inflation. And it turns out that inflation precisely drives the Universe in a state that corresponds to what is needed in order to make the hot Big Bang phase work.

Moreover, when gravity is described by general relativity, an accelerated expansion can be produced if the Universe content is dominated by a fluid with negative pressure. At energy scales relevant for inflation, field theory is the correct framework to describe matter. Since scalar fields are compatible with the symmetries of an homogeneous and isotropic expanding Universe, they are usually assumed to be responsible for the phase of inflation. Because their pressure is given by the difference between the kinetic energy and the potential energy it follows that, if the potential energy dominates over the kinetic energy, that is to say if the field slowly rolls down its potential, then a phase of inflation naturally takes place.

Inflation also provides a convincing explanation for the origin of the large scale structures in our Universe [3, 5]. In brief, the unavoidable vacuum quantum fluctuations of the coupled inflaton and gravitational fields are stretched to super-Hubble scales during inflation, where they undergo parametric amplification and, then, give rise to large scale structures and Cosmic Microwave Background (CMB) anisotropy. This part of the scenario is particularly interesting since it rests on the two pillars of modern physics, general relativity and quantum mechanics.

Inflation can take place at energies as large as 10^{16} GeV and clearly, at those energy scales, particle physics remains speculative since this corresponds to regimes that cannot be probed in accelerators. However, this has not prevented physicists to invent concrete models of inflation. In fact, this has rather caused the opposite problem, namely hundreds of different scenarios have been proposed, inspired by the various extensions of the particle physics standard model. Beyond the most simple models relying on a single slowly rolling scalar field, other possibilities include multiple field scenarios, possibly with non standard kinetic terms, non minimal coupling to the gravity sector, and/or potentials with localized features. Even the assumption that inflation is realized by means of scalar fields has been relaxed and setups involving vector fields or gauge fields have also been investigated. Facing this plethora of models the question of how the actual version of inflation can be identified then becomes a major issue.

Fortunately, these different scenarios do not all make the same predictions and, as a consequence, comparing them to cosmological data opens the possibility to identify the correct one. In this paper, we explore this route and show how this can be done with the recently released Planck data [6, 7, 8].

These data indicate that we live in a spatially flat universe, $|\Omega_K| < 0.005$ at 95% confidence level, which is very consistent with the idea that inflation took place in the early Universe. Moreover, the cosmological fluctuations are adiabatic (entropic modes are constrained to contribute less than a few percents) and Gaussian, $f_{\rm NL}^{\rm loc} = 0.8 \pm 5.0$, $f_{\rm NL}^{\rm eq} = -4 \pm 43$ and $f_{\rm NL}^{\rm ortho} = -26 \pm 21$ at 68% confidence level [9]. An important scientific result of the Planck mission [10] is the fact that a deviation from exact scale invariance has now been detected at a significant statistical level, namely $n_{\rm S} = 0.968 \pm 0.006$ at 68% confidence level, thus ruling out scale invariance at more than 5σ. In addition, the running has been found to be compatible with zero, $\mathrm{d}n_{\rm S}/\mathrm{d}\ln k = 0.003 \pm 0.007$ (with a pivot scale chosen at $k_* = 0.05\mathrm{Mpc}^{-1}$). All these observational facts are in agreement with the simplest models of inflation, namely those driven by a single scalar field, with a standard kinetic term, slowly rolling down its smooth potential.

As a consequence, the overall picture that emerges from the latest observational results is that the inflationary mechanism is non-trivial (i.e. the data are no longer compatible with an inflationary phase driven by a simple cosmological constant) but, at the same time, "non-exotic". In particular, the more complicated inflationary scenarios mentioned previously are now disfavored. Notice that this does not mean that they are ruled out, but simply that they are not needed to explain the data. In accordance with Occam's razor principle that the simplest viable explanation for the observations at hand ought to be preferred, it is thus appropriate to consider – at least for

the moment, and as long as the data do not force us to include more complicated setups – the simplest scenarios only, namely single-field slow-roll models with standard kinetic term. This type of scenarios is characterized by one free function, the potential $V(\phi)$. Therefore, identifying the "best model of inflation" is in fact equivalent to determining the potential $V(\phi)$ which best fits the data with the smallest number of free parameters and the least fine-tuning.

It should however be clear that, even if we restrict our considerations to this simple class of models, it still remains a very large number of possible scenarios [11]. Then comes the questions of how one can constrain these models, estimate their performances and rank them, in a statistically well-defined fashion, according to their performances in order to find "the best model(s) of inflation". Answering and discussing these questions is the main subject of the present paper.

This article is organized as follows. In section 2, we briefly review slow-roll inflation and its predictions. In section 3, we describe how the Bayesian model comparison approach can be used to discriminate between models that are competing to explain the data. We then apply this method to the case of inflationary models and present our results in section 4. Finally, in section 5, we summarize our main findings and discuss the prospects of future CMB missions.

2. Inflationary Predictions

The dynamics of a scalar field with a minimal kinetic term and a potential $V(\phi)$, living in a Friedmann-Lemaître-Robertson-Walker (FLRW) geometry, is described by a set of two equations, the Friedmann and Klein-Gordon equations. They are given by

$$H^2 = \frac{1}{3M_{\rm Pl}^2}\left[\frac{\dot{\phi}^2}{2} + V(\phi)\right], \qquad (1)$$

$$\ddot{\phi} + 3H\dot{\phi} + V_\phi = 0, \qquad (2)$$

where $H \equiv \dot{a}/a$ denotes the Hubble parameter, $a(t)$ is the FLRW scale factor and $\dot{a}$ its derivative with respect to cosmic time t. A subscript ϕ means a derivative with respect to the inflaton field, and $M_{\rm Pl}^2 = 1/(8\pi G)$ denotes the reduced Planck mass, G being the Newton constant. As already mentioned, the physics of this system is therefore fully specified by a single function $V(\phi)$, the shape of which should be constrained by means of observational data.

Inflation proceeds as long as the potential is flat enough, and when this is not the case anymore, inflation stops. The inflaton field then decays [12, 13], the products of which thermalize [14], and this is how inflation is smoothly connected to the standard hot Big Bang phase. The kinematics of this "reheating" epoch can be conveniently described by a single parameter, the so-called "reheating parameter" [15] defined by

$$\ln R_{\rm reh} \equiv \frac{1-3\bar{w}_{\rm reh}}{12\left(1+\bar{w}_{\rm reh}\right)}\ln\left(\frac{\rho_{\rm reh}}{\rho_{\rm end}}\right) + \ln\left(\frac{\rho_{\rm end}^{1/4}}{M_{\rm Pl}}\right). \qquad (3)$$

Here, $\rho_{\rm end}$ is the energy density at the end of inflation, $\rho_{\rm reh}$ is the energy density when reheating is completed and the radiation era begins, and

$$\overline{w}_{\rm reh} \equiv \frac{1}{N_{\rm reh}-N_{\rm end}}\int_{N_{\rm end}}^{N_{\rm reh}} \frac{p\left(n\right)}{\rho\left(n\right)}{\rm d}n \qquad (4)$$

is the averaged equation of state parameter over the number of e-folds $N \equiv \ln(a)$ of the effective fluid dominating the Universe during reheating. The knowledge of $R_{\rm reh}$ is necessary in order to work out the inflationary predictions for the CMB. Indeed, it allows us to relate the physical value of any length scale measured today to those during inflation. Within a completely specified model of inflation, $R_{\rm reh}$ therefore sets the location of the observational window. Physically, it depends on the mean equation of state parameter during reheating, and on the energy density at the onset of the radiation era, *ie* the first temperature the Universe ever acquired. At the microphysics level, reheating is clearly a very complicated phenomenon and it is maybe surprising that it can be described by just one or two parameters. But, in fact, the reheating parameter just measures the information that can be inferred on reheating from CMB data. The situation is similar to reionization. If one wants to describe this phenomenon with atomic physics, it is certainly very complicated but, as long as CMB predictions are concerned, the knowledge of one parameter, the optical depth, is sufficient to characterize it.

Let us now turn to the description of the inflationary perturbations. Since vector perturbations quickly decay during inflation, only two types of fluctuations

play a relevant role: density perturbations (scalar) and primordial gravity waves (tensor). The density perturbations are often described in terms of the Mukhanov-Sasaki gauge-invariant variable v, while h refers to gravity waves. In the Schrödinger picture, the quantum state of the cosmological perturbations are described by wavefunctionals, $\Psi[v(\boldsymbol{x})] \sim \Pi_{\boldsymbol{k}}\Psi\left(v_{\boldsymbol{k}}\right)$ and $\Psi[h(\boldsymbol{x})] \sim \Pi_{\boldsymbol{k}}\Psi\left(h_{\boldsymbol{k}}\right)$, where $v_{\boldsymbol{k}}$ and $h_{\boldsymbol{k}}$ denote the Fourier amplitudes of each type of fluctuations. They obey the Schrödinger equation where the Hamiltonian is obtained from a second order expansion of the total action. At this order, the Hamiltonian is quadratic and, hence, the solutions of the Schrödinger equation can be expressed in terms of Gaussian functions, namely

$$\Psi\left(v_{\boldsymbol{k}}\right) \propto e^{-\frac{\mathrm{i}}{2}\frac{f'_{\boldsymbol{k}}}{f_{\boldsymbol{k}}}v_{\boldsymbol{k}}^2}, \quad \Psi\left(h_{\boldsymbol{k}}\right) \propto e^{-\frac{\mathrm{i}}{2}\frac{g'_{\boldsymbol{k}}}{g_{\boldsymbol{k}}}h_{\boldsymbol{k}}^2}, \tag{5}$$

where a prime denotes derivative with respect to conformal time $\eta = \int \mathrm{d}t/a$, and where $f_{\boldsymbol{k}}$ and $g_{\boldsymbol{k}}$ are solutions of

$$f''_{\boldsymbol{k}} + \left[k^2 - \frac{\left(a\sqrt{\epsilon_1}\right)''}{a\sqrt{\epsilon_1}}\right] f_{\boldsymbol{k}} = 0\,, \tag{6}$$

$$g''_{\boldsymbol{k}} + \left(k^2 - \frac{a''}{a}\right) g_{\boldsymbol{k}} = 0\,. \tag{7}$$

As a consequence, studying cosmological perturbations during inflation boils down to solving Eqs. (6) and (7) with some initial conditions. A natural choice is the so-called "Bunch-Davies" vacuum. This is because, at the beginning of inflation, the physical wavelengths of the Fourier modes of cosmological relevance today are much smaller than the Hubble radius, and Eqs. (6) and (7) become $f''_{\boldsymbol{k}} + k^2 f_{\boldsymbol{k}} = g''_{\boldsymbol{k}} + k^2 g_{\boldsymbol{k}} = 0$. These modes do not feel spacetime expansion and, as a consequence, follow a Minkowski dynamics $f_{\boldsymbol{k}}, g_{\boldsymbol{k}} \simeq A_{\boldsymbol{k}}e^{ik\eta} + B_{\boldsymbol{k}}e^{-ik\eta}$. Since the quantum mean number of scalar particles is generically given by [16]

$$n_{\boldsymbol{k}} = \frac{i}{2k}\frac{f'_{\boldsymbol{k}}}{f_{\boldsymbol{k}}} - \frac{k + \frac{4}{k}\frac{f'^2_{\boldsymbol{k}}}{f^2_{\boldsymbol{k}}}}{4\Im\mathrm{m}\left(f'_{\boldsymbol{k}}/f_{\boldsymbol{k}}\right)} - \frac{1}{2}\,, \tag{8}$$

and a similar expression for tensors, the vacuum state for which $n_{\boldsymbol{k}} = 0$ corresponds to $f_{\boldsymbol{k}}, g_{\boldsymbol{k}} \propto e^{-ik\eta}$. As a consequence, the initial quantum states become $\Psi(v_{\boldsymbol{k}}) \propto e^{-kv_{\boldsymbol{k}}^2/2}$ and $\Psi(h_{\boldsymbol{k}}) \propto e^{-kh_{\boldsymbol{k}}^2/2}$, which indeed corresponds to the ground state of an harmonic oscillator with pulsation k.

At later time, the effective pulsation depends on the time profile of the background expansion through a and ϵ_1. For this reason, it is useful to introduce a hierarchy of slow-roll parameters according to [23]

$$\epsilon_{n+1} \equiv \frac{\mathrm{d}\ln|\epsilon_n|}{\mathrm{d}N}, \quad n \geq 0, \tag{9}$$

where $\epsilon_0 \equiv H_{\mathrm{ini}}/H$. The slow-roll regime takes place when all the ϵ_n's are much smaller than one. From this definition, one can see that, for density perturbations, the effective pulsation depends on ϵ_1, ϵ_2 and ϵ_3 while, for gravity waves, it only depends on ϵ_1. An important remark [17] is that, thanks to Eqs. (1) and (2), $H(N)$ and $V(\phi)$ are related through $V = M_{\mathrm{Pl}}^2 H(3H + \mathrm{d}H/\mathrm{d}N)$. It follows that the parameters ϵ_n can also be expressed in terms of the successive derivatives of the potential. In the slow-roll regime, $\epsilon_1 = -(\mathrm{d}H/\mathrm{d}N)/H \ll 1$ so that $V \simeq 3M_{\mathrm{Pl}}^2H^2$, and one has

$$\epsilon_1 \simeq \frac{M_{\mathrm{Pl}}^2}{2}\left(\frac{V_\phi}{V}\right)^2, \tag{10}$$

$$\epsilon_2 \simeq 2M_{\mathrm{Pl}}^2\left[\left(\frac{V_\phi}{V}\right)^2 - \frac{V_{\phi\phi}}{V}\right], \tag{11}$$

$$\epsilon_2\epsilon_3 \simeq 2M_{\mathrm{Pl}}^4\left[\frac{V_{\phi\phi\phi}V_\phi}{V^2} - 3\frac{V_{\phi\phi}}{V}\left(\frac{V_\phi}{V}\right)^2 + 2\left(\frac{V_\phi}{V}\right)^4\right] \tag{12}$$

and similar expressions for higher terms. The slow-roll approximation thus allows us to expand the solution to Eqs. (6) and (7) in these small parameters that can easily be calculated once the potential function $V(\phi)$ is known. One can then express the two-point correlation function of scalar and tensor fluctuations at the end of inflation, or, in Fourier space, the power spectra, according to [23, 18]

$$\mathcal{P}_\zeta(k) \equiv \frac{k^3}{4\pi^2 M_{\rm Pl}^2}\left|\frac{v_{\boldsymbol{k}}}{a\sqrt{\epsilon_1}}\right|^2 = \frac{H_*^2}{8\pi^2 M_{\rm Pl}^2 \epsilon_{1*}}\left[1-2(C+1)\epsilon_{1*}-(2\epsilon_{1*}+\epsilon_{2*})\ln\left(\frac{k}{k_*}\right)+\cdots\right], \quad (13)$$

$$\mathcal{P}_h(k) \equiv \frac{k^3}{2\pi^2}\left(\left|h_{\boldsymbol{k}}^+\right|^2+\left|h_{\boldsymbol{k}}^-\right|^2\right) = \frac{2H_*^2}{\pi^2 M_{\rm Pl}^2}\left[1-2(C+1)\epsilon_{1*}-2\epsilon_{1*}\ln\left(\frac{k}{k_*}\right)+\cdots\right]. \quad (14)$$

Here, the power spectra have been expanded around a pivot scale k_* and we have considered the two degrees of polarization $\pm$ of the graviton. The quantity $C \equiv \gamma_{\rm E} + \ln 2 - 2 \approx -0.7296$ is a numerical constant with $\gamma_{\rm E}$ being the Euler constant, and H_* and ϵ_{n*} denote the value of the function H and ϵ_n at the Hubble radius crossing time of the pivot scale during inflation.

For this simple class of models, establishing the inflationary predictions therefore ultimately comes down to calculating the quantities ϵ_{n*}. Because of Eqs. (10)–(12), ϵ_{n*} depend on $\theta_{\rm inf}$, the parameters characterizing the shape of the potential $V(\phi)$, and because reheating sets the time at which Eqs. (10)–(12) must be evaluated, one has $\epsilon_{n*} = \epsilon_{n*}(\theta_{\rm inf}, R_{\rm reh})$. As a consequence, if one can measure the power spectra (13) and (14), then one can constrain the parameters $\epsilon_{n*}(\theta_{\rm inf}, R_{\rm reh})$, which carry information about the shape of the potential and about reheating. In this manner, one can learn about inflation.

3. Bayesian Approach to Model Comparison

In the previous section, we have described how one can calculate the predictions of a given inflationary model. Now, we also would like to compare the performances of different inflationary scenarios and one way to carry out this program is to make use of the Bayesian approach to model comparison [19, 20]. Bayesian inference uses Bayes theorem to express the posterior probabilities of a set of alternative models $\mathcal{M}_i$ given some data set $\mathcal{D}$. It reads

$$p(\mathcal{M}_i|\mathcal{D}) = \frac{\mathcal{E}(\mathcal{D}|\mathcal{M}_i)\,\pi(\mathcal{M}_i)}{p(\mathcal{D})}. \quad (15)$$

Here, $\pi(\mathcal{M}_i)$ represents the prior belief in the model $\mathcal{M}_i$, $p(\mathcal{D}) = \sum_i \mathcal{E}(\mathcal{D}|\mathcal{M}_i)\pi(\mathcal{M}_i)$ is a normalization constant and $\mathcal{E}(\mathcal{D}|\mathcal{M}_i)$ is the Bayesian evidence of $\mathcal{M}_i$, defined by

$$\mathcal{E}(\mathcal{D}|\mathcal{M}_i) = \int {\rm d}\theta_{ij}\,\mathcal{L}(\mathcal{D}|\theta_{ij},\mathcal{M}_i)\,\pi(\theta_{ij}|\mathcal{M}_i), \quad (16)$$

where θ_{ij} are the parameters defining the model $\mathcal{M}_i$ and $\pi(\theta_{ij}|\mathcal{M}_i)$ is their prior distribution. The quantity $\mathcal{L}(\mathcal{D}|\theta_{ij},\mathcal{M}_i)$ represents the probability of observing the data $\mathcal{D}$ assuming the model $\mathcal{M}_i$ is true and θ_{ij} are the actual values of its parameters (likelihood function).

The posterior odds between two models $\mathcal{M}_i$ and $\mathcal{M}_j$ are then given by

$$\frac{p(\mathcal{M}_i|\mathcal{D})}{p(\mathcal{M}_j|\mathcal{D})} = \frac{\mathcal{E}(\mathcal{D}|\mathcal{M}_i)}{\mathcal{E}(\mathcal{D}|\mathcal{M}_j)}\frac{\pi(\mathcal{M}_i)}{\pi(\mathcal{M}_j)} \equiv B_{ij}\frac{\pi(\mathcal{M}_i)}{\pi(\mathcal{M}_j)}, \quad (17)$$

where we have defined the Bayes factor B_{ij} by $B_{ij} = \mathcal{E}(\mathcal{D}|\mathcal{M}_i)/\mathcal{E}(\mathcal{D}|\mathcal{M}_j)$. Under the principle of indifference, one can assume non-committal model priors, $\pi(\mathcal{M}_i) = \pi(\mathcal{M}_j)$, in which case the Bayes factor becomes identical to the posterior odds. With this assumption, a Bayes factor larger (smaller) than one means a preference for the model $\mathcal{M}_i$ over the model $\mathcal{M}_j$ (a preference for $\mathcal{M}_j$ over $\mathcal{M}_i$). In practice, the "Jeffreys' scale" gives an empirical prescription for translating the values of the Bayes factor into strengths of belief. When $\ln(B_{ij}) > 5$, $\mathcal{M}_j$ is said to be "strongly disfavored" with respect to $\mathcal{M}_i$, "moderately disfavored" if $2.5 < \ln(B_{ij}) < 5$, "weakly disfavored" if $1 < \ln(B_{ij}) < 2.5$, and the situation is said to be "inconclusive" if $\ln(B_{ij}) < 1$.

Bayesian analysis allows us to identify the models that achieve the best compromise between quality of the fit and simplicity. In other words, more complicated descriptions are preferred only if they provide an improvement in the fit that can compensate for the larger number of parameters. In the rest of this section, we illustrate how this idea works on a simple example.

Let $\mathcal{M}_1$ and $\mathcal{M}_2$ be two competing models aiming at explaining some data $\mathcal{D}$. Two parameters θ_1

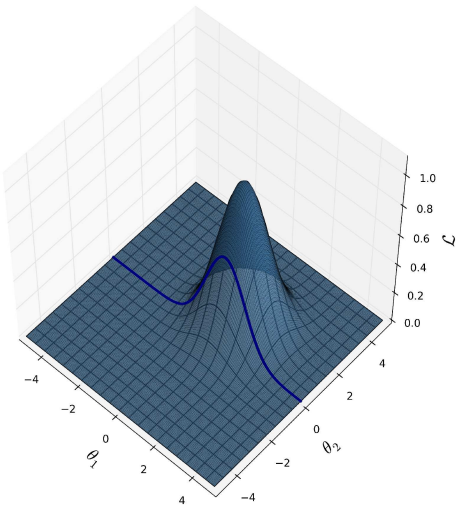

Figure 1 – Sketch of the likelihood for the toy model $\mathcal{M}_1$ discussed in section 3 (pale blue surface). The solid blue line corresponds to the likelihood of model $\mathcal{M}_2$, which is a sub-model of $\mathcal{M}_1$ with $\theta_2 = 0$.

and θ_2 describe the first model $\mathcal{M}_1$, and we assume that the likelihood function is a Gaussian centered at $(\bar{\theta}_1, \bar{\theta}_2)$ with standard deviations σ_1 and σ_2,

$$\mathcal{L}\left(\mathcal{D}|\theta_1,\theta_2,\mathcal{M}_1\right) = \mathcal{L}_1^{\max} e^{-\frac{(\theta_1-\bar{\theta}_1)^2}{2\sigma_1^2}-\frac{(\theta_2-\bar{\theta}_2)^2}{2\sigma_2^2}}. \tag{18}$$

This likelihood is represented in Fig. 1. We assume that the prior distribution on θ_1 and θ_2 is also a Gaussian, with standard deviations Σ_1 and Σ_2, and that the likelihood is much more peaked than the prior, that is to say $\Sigma_1 \gg \sigma_1$ and $\Sigma_2 \gg \sigma_2$. In this limit, Eq. (16) gives rise to a simple expression for the evidence of the model $\mathcal{M}_1$, namely

$$\mathcal{E}\left(\mathcal{D}|\mathcal{M}_1\right) = \frac{\sigma_1\sigma_2}{\Sigma_1\Sigma_2}\mathcal{L}_1^{\max}. \tag{19}$$

One can readily see that the higher the best fit, $\mathcal{L}_1^{\max}$, the better the Bayesian evidence which is, of course, expected. On the other hand, the ratio $\sigma_1\sigma_2/(\Sigma_1\Sigma_2)$ stands for the volume reduction in parameter space induced by the data $\mathcal{D}$ and, therefore, quantifies how much the parameters θ_1 and θ_2 must be fine tuned around the preferred values $\bar{\theta}_1$ and $\bar{\theta}_2$ to account for the data. From Eq. (19), it is thus clear that the larger this fine tuning, the worse the Bayesian evidence, the final result being a trade-off between both effects.

Now, let us imagine that the second parameter θ_2 is associated with some extra, non-minimal, feature (such as, say, isocurvature perturbations, non-Gaussianities, oscillations in the power spectrum, *etc*). We want to determine whether θ_2 (and, hence, the associated feature) is, at a statistically significant level, required by the data. To this end, we introduce the model $\mathcal{M}_2$ that is a sub-model of $\mathcal{M}_1$ where we choose $\theta_2 = 0$. This new model $\mathcal{M}_2$ has a single parameter θ_1. By definition, its prior distribution is Gaussian with standard deviation Σ_1 and its likelihood function is given by

$$\begin{aligned}\mathcal{L}\left(\mathcal{D}|\theta_1,\mathcal{M}_2\right) &= \mathcal{L}\left(\mathcal{D}|\theta_1,0,\mathcal{M}_1\right) &(20)\\ &= \mathcal{L}_1^{\max} e^{-\frac{\bar{\theta}_2^2}{2\sigma_2^2}} e^{-\frac{(\theta_1-\bar{\theta}_1)^2}{2\sigma_1^2}} &(21)\\ &\equiv \mathcal{L}_2^{\max} e^{-\frac{(\theta_1-\bar{\theta}_1)^2}{2\sigma_1^2}}, &(22)\end{aligned}$$

where we have defined the maximum likelihood for model $\mathcal{M}_2$ by $\mathcal{L}_2^{\max} = \mathcal{L}_1^{\max}\exp[-\bar{\theta}_2^2/(2\sigma_2^2)]$. This likelihood is displayed as the solid blue line in Fig. 1, and simply corresponds to the intersection of the full likelihood (18) with the plane $\theta_2 = 0$. In the same limit $\Sigma_1 \gg \sigma_1$ as before, the evidence for the model $\mathcal{M}_2$ is given by an expression similar to Eq. (19), namely $\mathcal{E}(\mathcal{D}|\mathcal{M}_2) = \sigma_1\mathcal{L}_2^{\max}/\Sigma_1$. The Bayes factor between models $\mathcal{M}_1$ and $\mathcal{M}_2$ therefore reads

$$B_{12} = \frac{\mathcal{L}_1^{\max}}{\mathcal{L}_2^{\max}}\frac{\sigma_2}{\Sigma_2} = e^{\frac{\bar{\theta}_2^2}{2\sigma_2^2}}\frac{\sigma_2}{\Sigma_2}. \tag{23}$$

The first term, $\mathcal{L}_1^{\max}/\mathcal{L}_2^{\max}$ represents the change in the best fit due to the fact that we have added new parameters. Obviously, the previous ratio is always larger than one since adding more degrees of freedom to describe the data can only improve the quality of the fit. On the other hand, the second term σ_2/Σ_2 represents the amount of fine tuning required for this new parameter θ_2 and is smaller than one. As a consequence, if the improvement of the fit quality is not large enough to beat fine tuning, one concludes that the parameter θ_2 is not required by the data. In the opposite case, one concludes that there is a statistically significant indication that $\theta_2 \neq 0$.

4. Results

In the previous section, we have explained why the performances of a model can be estimated by calculating its Bayesian evidence. We now apply this

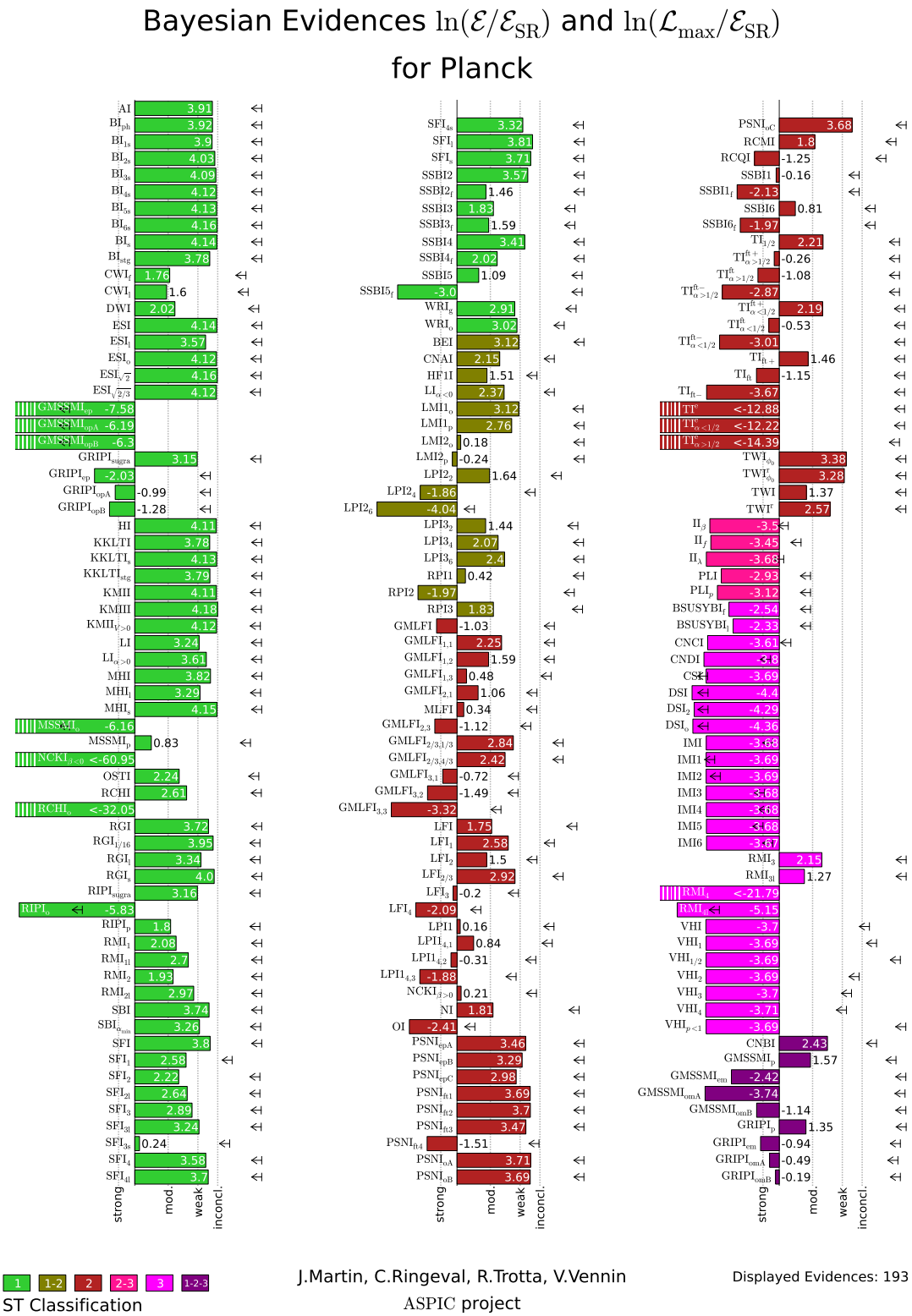

Figure 2 – Bayes factors (colored horizontal bars) and absolute upper bound to the Bayes factors (arrows) for the *Encyclopædia Inflationaris* inflationary scenarios, normalized to a vanilla slow-roll model. Figure taken from Ref. [21].

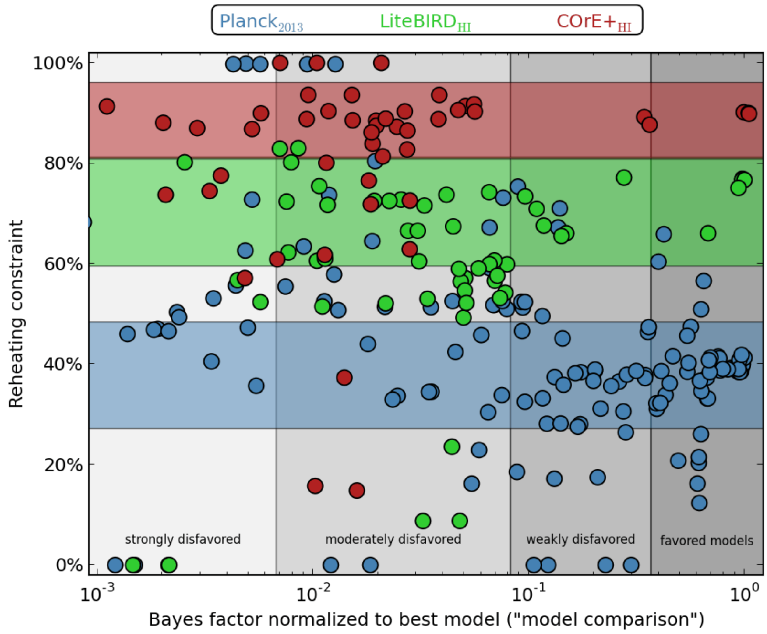

Figure 3 – Constraints on inflationary models in the space Bayesian evidence versus reheating prior volume reduction [24, 25]. The Planck data correspond to the blue circles (the models with too low Bayesian evidence are not displayed). The vertical shaded stripes stand for the four Jeffreys categories. The red and green circles represent the forecasted Bayesian evidence and reheating prior volume reduction for two future CMB missions, COrE+ and LiteBIRD, Higgs inflation being taken as the fiducial model to generate mock data.

technique to vanilla single-field inflationary models, the data set considered being the recently released Planck data.

In Fig. 2, following the work of Ref. [22], we display the Bayesian evidence of nearly 200 inflationary models taken from *Encyclopædia Inflationaris* [11]. Note that contrary to the numbers quoted in section 1, derived from the Planck 2015 results, Fig. 2 is obtained from the Planck 2013 data. However, the Planck 2015 data being completely consistent with those of 2013, the main conclusions will remain unchanged. The color code corresponds to the Schwarz–Terrero-Escalante classification [23], see Ref. [22] for further details.

This analysis reveals that about one third of the models can be considered as being ruled out ("strongly disfavored" in the Jeffreys scale). This gives an idea of the constraining power of the Planck data. Some of them are excluded because they provide a very poor fit to the data, while some of them are rejected because they require an extreme level of fine tuning. Among the most favored models ("inconclusive" in the Jeffreys scale), a large majority has "plateau" shaped potential. These include Khäler moduli inflation, Higgs inflation and the Starobinsky model, exponential SUSY inflation, brane inflation, KKLT inflation, loop inflation, *etc*. This confirms that the Planck data have the power to constrain the shape of the inflationary potential and, therefore, can provide information with regards to the physical conditions that reigned in the very early Universe.

The Planck mission has also the capability to constrain the reheating phase and we present the corresponding results in Fig. 3. The horizontal axis labels the Bayesian evidence, normalized to the best model, for the *Encyclopædia Inflationaris* inflationary models. Each of them is displayed as a blue color disk, the size of which has no specific meaning. Hence the best models are on the right ("favored models") and the worst are on the left ("strongly dis-

favored" models). The vertical axis, on the other hand, labels the fraction by which the prior volume for the reheating parameter introduced in Eq. (3) has been reduced by the data. When this is 0%, it means that the reheating parameter prior and posterior distributions are the same, and no information has been gained. Conversely, when this approaches 100%, it means that the posterior distribution is infinitely peaked and one has perfectly "measured" reheating. One can see that Planck leads to an average reduction of the reheating prior volume by 38% [25]. This means that, already with Planck, non trivial results about the kinematic properties of reheating can be obtained.

5. Conclusions

The analysis presented here explains how the CMB data can constrain the physics of the early universe in an efficient way. In very brief, Planck favors vanilla inflationary scenario and, within this class of models, is able to exclude one third of the scenarios and leads to a prior to posterior ratio reduction of about 40%.

The next generation of CMB missions, such as COrE+ or LiteBIRD, is currently being prepared and it is also interesting to discuss how the situation may evolve in the years to come. In Fig. 3, we have presented forecasted results for these two missions for the case where mock data are generated assuming Higgs inflation as the fiducial model. These experiments would typically allow us to exclude three quarters of the models [24]. This quantifies how much the constraining power of the data would increase in terms of model selection. In particular, one can see that while 51 models remain in the inconclusive zone with Planck, in the case discussed in Fig. 3, only 4 models would remain favored with LiteBIRD, and 2 with COrE+. One would therefore almost be able to identify *the* correct inflationary scenario. When it comes to reheating, the average reduction of the reheating prior volume would be 70% with LiteBIRD and 90% with COrE+ [25]. This means that one would be able to accurately measure the reheating parameter. In other words, inflationary Bayesian model comparison and reheating exploration are now also entering the "precision cosmology" epic.

References

[1] A. Starobinsky, *PLB*-91-99-1980.
[2] A. Guth, *PRD*-23-347-1981.
[3] V. Mukhanov and G. Chibisov, *Jetp*-33-532-1981.
[4] A. Linde, *PLB*-108-389-1982.
[5] A. Starobinsky, *PLB*-117-175-1982.
[6] Planck Collaboration, arXiv:1502.01582.
[7] Planck Collaboration, arXiv:1502.02114.
[8] Planck Collaboration, *A&A*-2014-571-A22.
[9] Planck Collaboration, arXiv:1502.01592.
[10] Planck Collaboration, arXiv:1502.01589.
[11] J. Martin, C. Ringeval, and V. Vennin, *Phys.Dark Univ.* 2014-01-003.
[12] M. Turner, *PRD*-28-1243-1983.
[13] L. Kofman, A. Linde and A. Starobinsky, *PRD*-56-3258-1997.
[14] D. Podolsky, G. Felder, L. Kofman and M. Peloso *PRD*-73-023501-2006.
[15] J. Martin and C. Ringeval, *PRD*-82-023511-2010.
[16] J. Martin, V. Vennin and P. Peter, *PRD*-86-103524-2012.
[17] V. Vennin, *PRD*-89-083526-2014.
[18] J. Martin, C. Ringeval and V. Vennin, *JCAP*-1306-021-2013.
[19] M. Kunz, R. Trotta and D. Parkinson, *PRD*-74-023503-2006.
[20] R. Trotta, *Contemp*-49-71-2008.
[21] J. Martin, C. Ringeval, R. Trotta, and V. Vennin, *PRD*-90-063501-2014.
[22] J. Martin, C. Ringeval, R. Trotta and V. Vennin, *JCAP*-2014-1403-039.
[23] D. Schwarz and C. Terrero-Escalante, *JCAP*-0408-003-2004.
[24] J. Martin, C. Ringeval and V. Vennin, *JCAP*-1410-038-2014.
[25] J. Martin, C. Ringeval and V. Vennin, *PRL*-8-114-081303-2015.